Eur Biophys J (1987) 15: 169–176

European Biophysics Journal

Reassembly of brome mosaic virus from dissociated virus

A neutron scattering study

M. Cuillel[1], C. Berthet-Colominas*[1], P. A. Timmins[2], and M. Zulauf[1]

[1] European Molecular Biology Laboratory and [2] Institut Laue-Langevin, 156X, F-38042 Grenoble Cedex, France

Received December 5, 1986/Accepted in revised form April 30, 1987

Abstract. The reconstitution of Brome Mosaic Virus (BMV) has been studied using neutron scattering. Experiments were performed on disassembled virus without subsequent separation of components. Phase diagrams of the disassembly and subsequent reassembly of BMV were established as a function of pH and LiCl molarity by analytical centrifugation and quasi-elastic light scattering. Disassembly occurs at a pH above 6.5 and above 0.8 *M* LiCl. On reassembly, if the pH is lowered first, capsids are formed without subsequent incorporation of RNA. Neutron scattering was used to investigate the formation of virus particles, when the ionic strength was lowered from 1.4 to 0.1 *M* LiCl at pH 7.8. The reconstitution was followed continuously. As it was driven by a lowering of the ionic strength the kinetics of the process cannot be studied for short times. However the fact that at any given ionic strength no evolution of the scattering was observed with time implies that the reconstitution is complete within a few minutes. The observations in buffers with various amounts of D_2O lead to the conclusion that the reassembly is achieved by co-condensation of the RNA and of the capsid proteins.

Key words: Plant virus, neutron scattering, self-assembly

Introduction

Self-assembly is believed to be one of the key steps in the morphogenesis of small plant viruses. In the case of the simple icosahedral plant viruses much is known on the structure of the assembled particle. Indeed the structures of three of these viruses, Tomato bushy stunt virus (TBSV) (Harrison et al. 1978), Southern bean mosaic virus (SBMV) (Abad-Zapatero et al. 1980) and Satellite tobacco necrosis virus (STNV) (Liljas et al. 1982) have been determined by X-ray crystallography to better than 3 Å resolution at least for the major part of the protein coat. Despite this detailed knowledge, the pathway (or pathways) of assembly are very poorly understood. It is clear, however, that the assembly process must be mediated by a variety of interactions, in particular protein-protein and protein-RNA. The importance of these two types of interaction is not the same for all the spherical viruses. Turnip Yellow Mosaic Virus (TYMV), is a virus having strong protein-protein interactions, whereas in Cucumber Mosaic Virus (CMV), protein-RNA interactions are predominant. Moreover Jacrot et al. (1977) have noted that there appears to be a correlation between the strength of protein-RNA interaction and the depth of interpenetration of protein into the RNA core.

Brome mosaic virus (BMV) is an example of an icosahedral plant virus having strong enough protein-protein interactions to form, under certain conditions, empty capsids in the absence of RNA (Pfeiffer and Hirth 1974) but with sufficiently strong protein-RNA interactions to stabilise the virus under conditions where the empty capsids would be dissociated. BMV is composed of 180 subunits of molecular weight 20,300, arranged on a $T = 3$ icosahedral surface lattice, surrounding a divided genome. The four pieces of RNA (Mr 1.09; 0.99; 0.70; 0.28×10^6) are encapsidated in three virions with an RNA content of about 10^6 daltons in each. The RNA-protein interactions in the virus have been studied in some detail using nuclear magnetic resonance spectroscopy (Vriend et al. 1982) and cross-linking techniques (Sgro et al. 1986). In order to better understand the self-assembly process, we have studied by X-ray scattering the reassembly of BMV protein into empty capsids in the absence of RNA (see companion paper: Berthet-Colominas et al. 1987). This study showed that the capsids were constructed by the sequential addition of oligomeric protein subunits and that at any particular stage of the

* To whom offprint requests should be sent

process a wide range of aggregates was present. Here we report a similar study using neutron scattering to investigate the reassembly of virus from protein and RNA by change of ionic strength. Neutron scattering is particularly well adapted to this problem as by using the D_2O/H_2O contrast variation technique (Jacrot 1976) we can follow the evolution in size and mass of either the RNA or protein moiety in the presence of the other. In our case experiments at 68% D_2O were particularly useful, as at this contrast contributions from RNA scattering are minimized and the complexity of the system is reduced. It has been known for a long time (Kelly 1962a; Yamazaki and Kaesberg 1963a, b; Kaper et al. 1965) that some spherical plant viruses can be easily dissociated in the presence of high concentrations of monovalent or divalent salts. This is the case for BMV at least at high pH. Whereas divalent salts often precipitate the RNA, monovalent salts yield solutions in which disassembled protein subunits and RNA coexist. The most efficient salt that we have tested i.e. the salt which achieves dissociation at the lowest concentration, is LiCl. Using this salt, phase diagrams of the disassembly and reassembly processes were first established by analytical sedimentation and quasi-elastic light scattering studies, in order to define precisely the pH and ionic strength conditions for well defined pathways of these processes. Reassociation was carried out on dissociated products of the virus without separation or purification of the components. A reassembly pathway with high yield of complete virions was then chosen and the condensation of protein onto RNA was characterized by neutron scattering experiments performed while the assembly proceeded spontaneously.

Material and methods

BMV was multiplied on barley and purified as described by Pfeiffer and Hirth (1974).

Virus dissociation was obtained by 2 procedures: *(1)* change of pH at constant ionic strength by adding to the virus suspensions (4 mg/ml; 0.01 *M* sodium acetate; 0.001 *M* EDTA; 1.6 *M* LiCl; pH 4.7) a superceding titrant (0.2 *M* *Tris*-HCl; 1.6 *M* LiCl; pH 8.8) to define the final pH. *(2)* Change of ionic strength at constant pH by adding to virus suspensions (4 mg/ml; 0.05 *M* sodium cacodylate; 0.05 *M* LiCl at a given pH), a high LiCl titrant (0.05 *M* sodium cacodylate; 6 *M* LiCl). Reconstitution was carried out as follows: a virus solution was first dissociated as described above by bringing it to a final pH 7.8 and 1.6 *M* LiCl, and then dialysed into a solution containing 0.005 *M* $MgCl_2$ at the desired pH and ionic strength. The ionic strength, expressed as LiCl molarity, was estimated from a measurement of the conductivity. Mixing experiments performed in the presence or absence of virus revealed that in no case did the viral constituents affect the solution conductivity in an appreciable way as long as the LiCl concentration exceeded 0.1 *M*.

For the radioactivity assays BMV was ^{14}C labelled by reductive protein methylation with ^{14}C formaldehyde at pH 6 as described by Sgro et al. (1986). Dissociated virus solutions were analysed on sucrose gradients as follows: 4 mg of dissociated virus was loaded on a 11 ml 10–35% sucrose gradient in *Tris* buffer (0.01 *M* *Tris*, 1.6 *M* LiCl, 0.005 *M* $MgCl_2$, pH 7.8) and centrifuged in a SW 41 Spinco rotor for 19 h at 39,000 rpm. The gradient was fractionated from the top with a Buchler Auto Densi Flow II. The optical density at 260 nm and the radioactivity for each fraction were plotted against the fraction number.

Hydrodynamic measurements

The analytical centrifuge used was a MSE Centriscan 75 equipped with Schlieren optics. The sedimentation coefficients are reported in reduced form as S_{20w}, i.e. corresponding to 20°C and the viscosity of water. Photon correlation experiments were performed using an argon laser (Spectra Physics) and a 96 channel digital auto correlator (Malvern Precision Instruments) in a set-up and with procedures as described previously (Cuillel et al. 1983b). The measured diffusion coefficients are also quoted in their reduced form.

Electron micrographs were taken on a Jeol 100 CX. Samples were negatively stained with 1% uranyl acetate.

Neutron scattering

Dissociated virus solutions at pH 7.8, 6 *M* LiCl (obtained as described above) were first dialysed into a buffer of the same salt concentration and the same pH containing different amounts of D_2O (0%, 20%, 68%, 90%). Samples were then dialysed into a unique reconstitution buffer having the same amount of D_2O (0.01 *M* *Tris*, 0.005 *M* $MgCl_2$, 0.01 *M* LiCl, pD 7.40) for the time necessary to reach the required ionic strength. The pH of the deuterated buffer was corrected and corresponded to $pD = pH + 0.3314\,n + 0.0766\,n^2$; $n = D_2O$ mole fraction in the solvent. This was achieved by pumping the measuring solution and the dialysate through an exchange cell in which the two liquids remained separated by a dialysis membrane. The membrane area was about 10 cm^2. The set-up is shown schematically in Fig. 1. The conductimetry cell allowed the ionic strength of the solution to be monitored continuously. The cell was previously

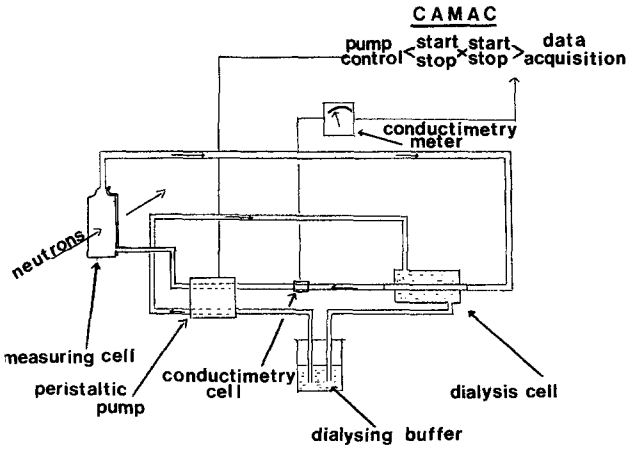

Fig. 1. Schematic view of the set-up used in neutron scattering experiments allowing investigation of a single sample at various stages of dialysis towards low ionic strength. Two closed circuits containing sample and dialysate buffer are pumped through the dialysis cell where they remain separated by dialysis tubing. A conductimetry cell in the sample circuit allows measurement of the ionic strength reached after pumping for a given time. Pumping is then discontinued (under computer control) and the scattering experiment performed on the sample aliquot in the measuring cell. After exposure pumping is resumed to obtain a new value of ionic strength

calibrated with solutions containing LiCl between 1.5 M and 0.01 M, allowing the monitoring of the progress of dialysis as well as the stability of the ionic strength during the neutron measurements.

The sequence for neutron scattering measurements was the following:

A first scattering curve was recorded at an ionic strength such that the virus was dissociated (1.4 M LiCl, pD = 7.40). The measurement time was around 10 min.

This was followed by either the start of a second data acquisition in order to check a possible evolution of the scattering curve with time, or the start of the peristaltic pump P initiating a dialysis against the 0.01 M LiCl pD = 7.40 buffer. When the conductimetry cell reached the required value the dialysis was stopped, simultaneously starting the next neutron measurement. The dialysis time varied between 3 min at high ionic strength and 9–10 min at the final ionic strength. Measurements were performed on the small-angle scattering instrument D11 (Ibel 1976) at the Institut Laue-Langevin, with a sample-detector distance of 5 m and a wavelength of 6 Å. With these conditions the range of the scattering vector ($Q = (4\pi/\lambda)\sin\theta$; 2θ = scattering angle) attainable was from 0.01–0.055 $Å^{-1}$.

Data analysis

The spectra were analyzed by modelling the virus as a spherical particle consisting of two concentric shells with different scattering densities corresponding to RNA and protein (Zulauf et al. 1981). Dissociated material was roughly approximated by a flat background. This analysis served to assess for changes of the viral geometry in response to changes of the ionic strength, and also to obtain estimates of $I(0)$ the intensity scattered at zero angle. The intensity $I(0)$ per unit concentration, corrected as usual for sample transmission and cell thickness, is directly proportional to the square of the scattering length of the scatterers. If these are completely assembled virions comprising 90 dimers and RNA, then

$$I_{\text{assembled}}(0) = \alpha\,[90\,(\Sigma b - \varrho V)_{\text{dimer}} + (\Sigma b - \varrho V)_{\text{RNA}}]^2$$
$$= \alpha\,[90\,M_{\text{dimer}}\,\bar{\varrho}_{\text{protein}} + M_{\text{RNA}}\,\bar{\varrho}_{\text{RNA}}]^2 .$$

Here Σb is the sum of the scattering lengths of all nuclei of the constituent moiety, V the corresponding "dry" volume and ϱ the scattering length density of the buffer. The reduced excess densities $\bar{\varrho}$ are defined by

$$\bar{\varrho} = (\Sigma b - \varrho V)/M$$

and have characteristic values for the two moieties, rather independent of the particular amino acid or base composition (Jacrot 1976):

$$\left.\begin{aligned}\bar{\varrho}_{\text{protein}} &= (2.95 - 7.11\,\chi)\,10^{-14}\,\text{cm/dalton}\\ \bar{\varrho}_{\text{RNA}} &= (3.74 - 5.18\,\chi)\,10^{-14}\,\text{cm/dalton}\end{aligned}\right\}\ \text{where}$$

$$\chi = \frac{[D_2O]}{[H_2O]}.$$

Similarly, if the virions are completely dissociated into 90 free dimers and the 4 species of RNA with weights $M_1 \ldots M_4$, we have

$$I_{\text{dissociated}}(0) = \alpha\,90\,M_{\text{dimer}}^2\,\bar{\varrho}_{\text{protein}}^2$$
$$+ \alpha\,(\tfrac{1}{3}M_1^2 + \tfrac{1}{3}M_2^2 + \tfrac{1}{6}M_3^2 + \tfrac{1}{6}M_4^2)\,\bar{\varrho}_{\text{RNA}}^2 .$$

Using the values of $\bar{\varrho}$ given above we obtain

$$I_{\text{assembled}}(0) = \alpha\,(14.36 - 30.78\,\chi)^2\,Å^{-2},$$
$$I_{\text{dissociated}}(0) = \alpha\,(4.41 - 7.26\,\chi)^2\,Å^{-2}.$$

Suppose the intensity of a native virus solution has been measured in one single contrast. The scale factor α in the above expressions can then be calculated, and we can predict $I(0)$ in all other contrasts, both for disassembled and assembled virus. In our reconstitution experiments we assume that our solutions contain predominantly assembled and completely disassembled virions, but no intermediates or other states of aggregation. The observed intensity can then be expressed as

$$I_{\text{observed}}(0) = y\,I_{\text{assembled}}(0) + (1 - y)\,I_{\text{dissociated}}(0)$$

and the fraction y of intensity due to reassembled particles can thus be calculated.

Results

Disassembly phase diagram

The dissociation states of BMV as a function of pH and LiCl ionic strength (the LiCl molarity will be designated by I below) were investigated in the following way: Native BMV was dissolved in a solution in which it remained undissociated. I or pH were then changed by mixing a titrant into the solution such as to obtain the desired final values of I and pH (see Material and methods). After equilibration the solutions were analysed by measuring sedimentation velocities (analytical centrifugation) and in some instances their diffusion constants (quasi elastic light scattering). No attempt was made to estimate, from the height of the sedimentation peaks, the amount of aggregates migrating with a particular velocity.

In the phase diagram obtained in this way we can distinguish three different regions limited by a range of pH and ionic strength. Inside each region we found the protein and RNA in a particular and well-defined state allowing the establishment of well-defined boundaries to delimit these zones, as shown in Fig. 2 a. Pathways of dissociation are shown by arrows, with the initial reassembly condition indicated by an asterisk. In zone 1 the virus is undissociated and may be compact ($S = 84$, $D = 1.57 \times 10^{-7}$ cm^2/s), or slightly swollen (up to $S = 78$, $D = 1.46 \times 10^{-7}$ cm^2/s). This phenomenon of swelling has been studied extensively in the past (Incardona et al. 1964; Pfeiffer and Durham 1977; Zulauf 1977) and is not further considered here. Although zone 2 is somewhat heterogeneous, it contains essentially free RNA and empty capsids. The capsids have $S = 50 \pm 1$; $D = 1.30 \times 10^{-7}$ ($M = 3.6 \times 10^6$) and lead to well defined sedimenting peaks and almost unperturbed single exponentials in quasielastic light scattering experiments. These capsids do not exist for pH > 6.5 and $I < 1.0$. In zone 3, the virus is dissociated into RNA and low molecular weight protein (monomers, dimers, and some oligomers; Cuillel et al. 1983 b). In analytical centrifugation the fast migrating peak due to the capsids has disappeared. Due to the polydispersity of the sample the light scattering leads to correlation functions comprising several exponentials.

The efficiency of the dissociation in zone 3 was further investigated using virus with ^{14}C-labelled protein (Material and methods). The viral components were separated on a sucrose gradient; radioactivity was found essentially with the protein fraction as shown in Fig. 3.

Phase diagram of reassembly

Figure 2 a shows that complete dissociation of BMV into its components can be obtained at elevated values of ionic strength and pH. We have chosen an arbitrary point well inside zone 3 of Fig. 2 a as a starting point for our reassembly experiments, viz. $I = 1.6$, pH 7.8 (see Material and methods). A solution containing virus at 4 mg/ml in these conditions was then dialysed into buffers of various final values of I and pH, and the dialysed solutions were characterized by sedimentation and diffusion as before. Thus a reassembly

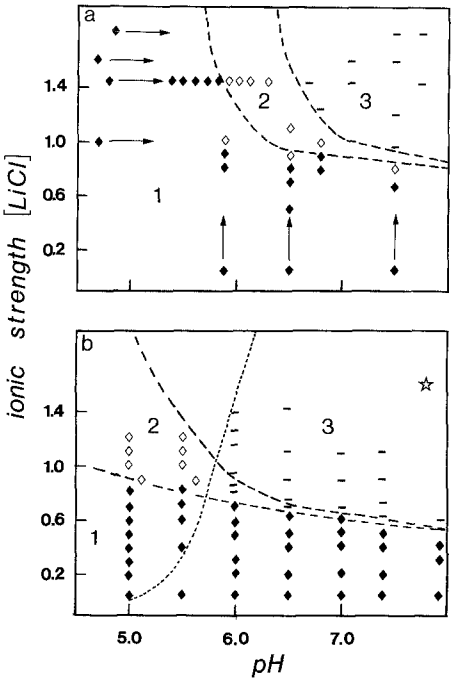

Fig. 2 a and b. Phase diagrams for disassembly (**a**) and reassembly (**b**) of BMV, delimiting regions denoted by encircled figures of defined states as explained in the text. The asterisk indicates the starting condition, and the arrows show the changes of parameters. The figures in (**b**) denote characteristic S-values found in these regions

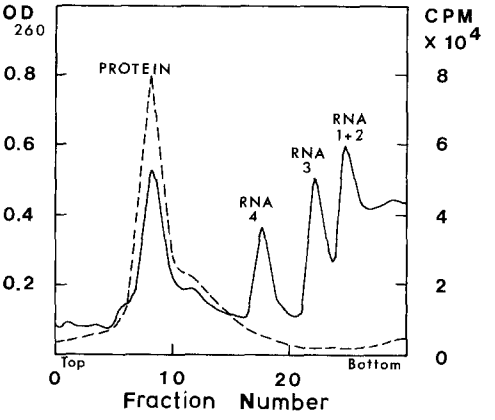

Fig. 3. Fractionation of dissociated BMV radioactively labelled at pH 7.4, 1.6 M LiCl obtained in a sucrose gradient. The full curve shows OD at 260 nm of the fractions collected, and the broken curve the corresponding radioactivity

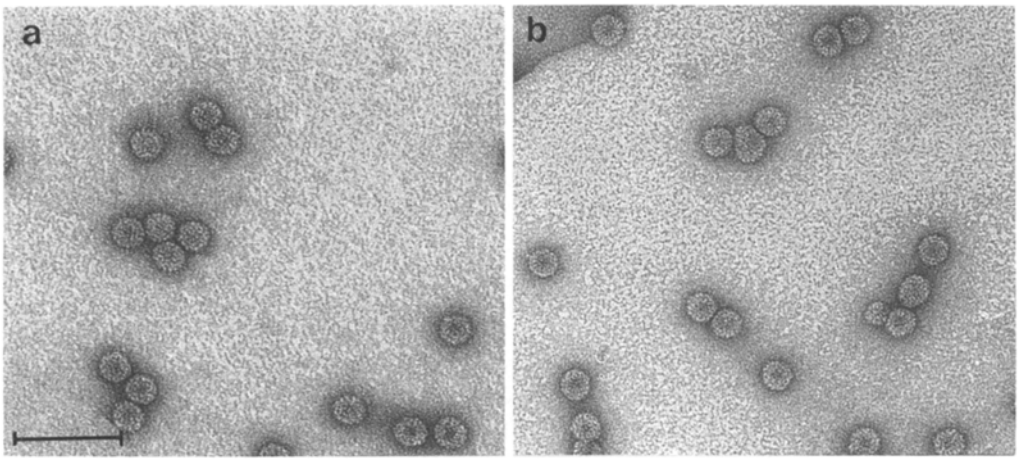

Fig. 4 a and b. Electron micrographs of native (**a**) and reconsituted (**b**) BMV both at pH 7.4 and 0.1 *M* LiCl. Samples are negatively stained. The bar length correspond to 100 nm

phase diagram could be established. Figure 2 b shows this diagram. Three zones can be distinguished, obtained by pathways in which the starting point (asterisk) is connected directly with each point in the diagram. Zone 3 is characterized by no reassociation between RNA and protein. The corresponding solutions show features similar to those discussed for zone 3 of the dissociation phase diagram. Zone 2 is an intermediate zone. At higher pH (right hand branch), coexistence of virions ($\sim 75\,S$) with dissociated material is observed, whereas at low pH, capsids may form ($52\,S$). Once formed, these capsids are incapable of RNA uptake when I is further reduced below 0.8. Zone 1 is characterized by well-defined sedimentation peaks and single exponentials in quasi-elastic light scattering experiments. The virions formed at pH > 6.5 correspond more closely to the native virus in its swollen form in the presence of Mg^{2+} (Zulauf 1977). This is corroborated by the following findings: *(i)* electron micrographs of reassembled and native virus in this domain are indistinguishable (Fig. 4); *(ii)* from $S_{20w} = 80$ and $D_{20w} = 1.51 \times 10^{-7}$ a molecular weight of 4.6×10^6 is obtained; *(iii)* when the reconstitutions at pH 7.5 $I = 0.1$ are dialysed to pH 5.0, a slight contraction of the virions to $S_{20w} = 84$, $D_{20w} = 1.57 \times 10^{-7}$ is observed, as found in the corresponding swelling experiments on BMV performed without dissociation of the virus (Zulauf 1977).

Neutron scattering

Neutron scattering experiments were designed to detect the onset of virus formation and to follow its ionic strength dependence. To this end, a solution at pH 7.8, was examined at different values of the ionic strength between 1.4 and 0.1 *M* LiCl as described in Material and methods. The scattering curves were corrected for

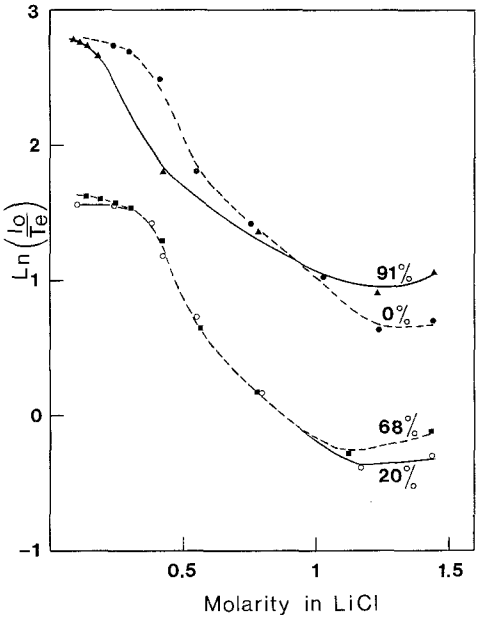

Fig. 5. Neutron intensity at $Q = 0$ as a function of the ionic strength. I (0) is corrected for the transmission (T) and thickness (e) of the sample and normalised to the incoherent scattering of water. The ionic strength is given in LiCl molarity

solvent and background scattering and normalised to the incoherent scattering of water. The intensity at $Q = 0$, (I (0)), was determined by Guinier analysis. The variation of I (0) as a function of the final ionic strength for different percentages of D_2O/H_2O is shown in Fig. 5. The values of I (0) vary as expected with contrast and the efficiency of the reconstitution as well as the value of the ionic strength at which the process starts are similar. The increase of the intensity with decreasing ionic strength could be due either to the increase in the size of the particles (addition of protein subunits to the RNA) or to the increase in the number

of high molecular weight particles (e.g. virus particles). The third possibility would be the formation of empty capsids followed by incorporation of RNA.

The qualitative evolution of the scattering curves corresponding to different contrasts can help us to distinguish between these possibilities. Figure 6 shows this evolution for 68% D_2O/H_2O and 0% D_2O/H_2O. At 68% D_2O, the RNA is "invisible" for neutrons and the scattering is dominated by the protein. If all the protein were present as dimers, the scattered intensity would decay only very slowly and monotonically in the Q-range shown. However, the data for $I = 1.4$ show a distinct peak centred around $Q = 0.035\,\text{Å}^{-1}$ indicating that the dissociation was not complete (96% dissociation) i.e. there remained a small proportion of virions in the solution at the beginning of the reconstitution (the 4% of undissociated virus is consistent with the sedimentation results which would not be able to detect this amount of virus). Upon lowering the ionic strength, this peak becomes more and more prominent; at the same time the intensity at low angles increases, whereas the asymptotic intensity towards high Q-values decreases. The position of the minimum does not change indicating that during the process the diameter of the spherical particles does not vary appreciably. The 68%D_2O/H_2O curve does not enable us to distinguish between virions or empty capsids as at this contrast the RNA contributes very little to the scattering.

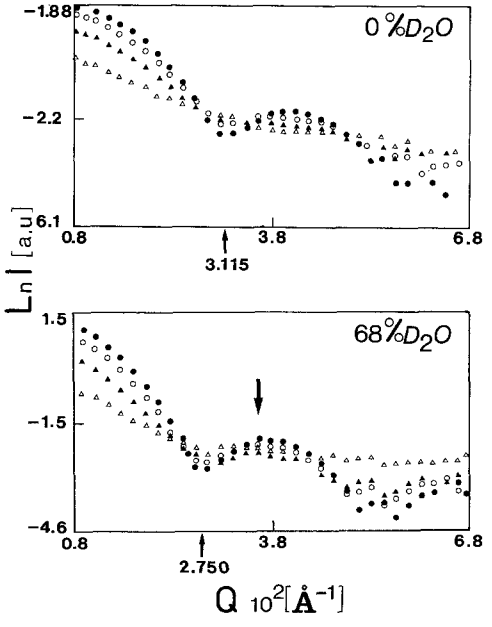

Fig. 6. Logarithm of the scattered neutron intensity, $\ln I(Q)$, as a function of the scattering vector Q in reassembly experiments at various LiCl concentrations in 0% D_2O and 68% D_2O. ●—● 0.2 *M* LiCl, ○—○ 0.4 *M* LiCl, ▲—▲ 0.6 *M* LiCl, △—△ 1.4 *M* LiCl

A set of curves at another contrast is then necessary. The variation (with the ionic strength) of the 0% D_2O/H_2O curves is similar to that in 68% D_2O. The differences are in the values of the intensities (larger in 0% D_2O) and in the position of the first minimum (Q_{min}). The values of Q_{min} observed are $3.11 \times 10^{-2}\,\text{Å}^{-1}$ for 0% and $2.75 \times 10^{-2}\,\text{Å}^{-1}$ for 68% D_2O. The set of curves corresponding to 90% D_2O has a $Q_{min} = 3.0 \times 10^{-2}\,\text{Å}^{-1}$, whereas the low signal at 20% D_2O prevents the determination of a precise value of Q_{min}. Furthermore the values of Q_{min} observed correspond to a spherical particle with the dimensions corresponding to those found for the BMV in a swollen state (Zulauf 1977; Incardona et al. 1973). It is precisely this difference in the Q_{min} which shows that the particles in the solution are virions rather than empty capsids. If the reconstituted particles were empty capsids the curves obtained in 68% and 0% would be identical. This finding together with the fact that within a set of curves the Q_{min} remains unchanged leads us to conclude that the increase in the $I(0)$ values (Fig. 6) corresponds to the number of virions increasing concommittantly with a decrease in the amount of dissociated virus.

Therefore, we can assume that at any point in the experiment the solution was composed of dissociated protein, nucleic acid and virions, the relative amount of these particles changing with the ionic strength. At high ionic strength only a very small amount of virions was present, most of the material was dissociated; on lowering the ionic strength more and more virions were reconstituted. The scattering of the swollen native virus alone can be measured, and by procedures which have been explained previously (see, e.g. Zulauf et al. 1981), it can be modelled in the Q-range considered, by a single homogeneous protein shell with inner and outer radii of 95 and 143 Å, respectively (Schneider et al. 1978; Zulauf et al. 1981). The scattering of dissociated protein has been measured previously (Cuillel et al. 1983b); in the Q-range considered here, the intensity varies little and can be reasonably well approximated by a constant. Thus, the observed scattering can be modelled by a shell structure superposed on a flat background, by varying uniquely the model scale factor and the background. Fits are shown for 2 cases in Fig. 7, and it is seen that they describe the data satisfactorily. It follows a posteriori that our hypothesis is valid, viz. that viral geometry is independent of ionic strength, and also that no other intermediates or aggregates are present. In order to estimate the number of newly formed virions as a function of ionic strength, we can use the calculated extrapolations for $I(0)$ from the model fits and compare them with expected values for completely dissociated and completely assembled virus. The latter can be calculated from intensity measurements of native virus in any

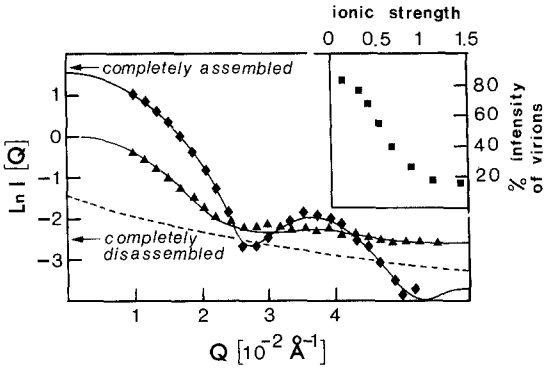

Fig. 7. Fits of the model described in the text corresponding to 68% D_2O at the ionic strength indicated. Model permits extrapolation to $Q = 0$ as shown. *Dashed line* represents neutron scattering curve of the protein at neutral pH. It corresponds to the completely dissociated structure for the percentage 68% D_2O where the RNA is matched. The insert shows the percentage of intensity I (0) corresponding to complete virus particles, as obtained from the fits at all ionic strengths

contrast, as explained in Material and methods and shown by the arrows in Fig. 7. We can then calculate, for each ionic strength, the percentage of virus assembly, expressed as a percentage of the intensity scattered by the viruses present in the solutions. The results are shown in the insert of Fig. 7. At high ionic strength, roughly 20% of the scattered intensity is due to undissociated virus. On a weight basis, this corresponds to only about 4% of the total material which is still organized as viruses, and thus cannot be detected by analytical ultracentrifugation. At low ionic strength, over 80% of the scattered intensity stems from viruses. The reconstitution yield is therefore around 40% w/w. The curve in the inset is of sigmoidal shape, but its asymptotic branch towards low I is not well measured. The reconstitution yield is therefore only a crude estimate. However, the midpoint of the curve lies around 0.6 M LiCl, as expected from the phase diagram.

Discussion

Both the dissociation and the reassembly phase diagram of BMV (Fig. 2a and b) show that a transition from virus to disassembled constituents or vice versa can be obtained at pH above 6.5 by changing the ionic strength, which is produced in these in vitro experiments by the concentration of LiCl. Evidently these ions interfere with the protein/RNA interactions. Provided the pH is kept higher than 6 any decrease of the ionic strength results in a reconstitution of the virus (zone 1). At high ionic strength the phosphate groups of the RNA and the protein charges are strongly shielded by counterions and the protein subunits rarely "see" the RNA. Upon lowering the ionic strength this shielding decreases enabling electrostatic interactions between the two types of molecules. These strong interactions could create a centre of attraction of the protein around the RNA, facilitating the interactions between the subunits. This process can be viewed as a protein condensation on the RNA. The precise control of the number of subunits required to form an empty capsid revealed by the study of the capsid self-assembly phenomenon (Cuillel et al. 1983a; Berthet-Colominas et al. 1986) leads to the assumption that the interactions between proteins also regulates this parameter in the virus reconstitution. Even if the pH is near neutrality and consequently the carboxyl-carboxylate interactions are reduced by the ionisation of the carboxyl groups the number of monomers in a reconstituted virus is precisely regulated.

The condensation of the dimers around the RNA was further corroborated by the neutron scattering results. As shown in Fig. 6 at each ionic strength value the first and second minima and the second maximum of the scattering curve occur at the same Q values. The positions of these features are known to indicate that the geometry of the scattering particles e.g. their radius and internal structure, remains unchanged.

Due to the experimental protocol (change of ionic strength during several minutes followed by recording of the scattering curve for some ten minutes) we can follow the reconstitution as a function of the time only if it takes place on a time scale longer than several minutes. We can thus deduce from the fact that once the ionic strength is fixed the scattering curve does not change with time, that the formation of virions is completed in less than 10 min at all ionic strengths.

The major conclusion of our work is that a change in the ionic strength is followed by an increase of the number of reconstituted virions rather than in the completion of incomplete particles. Alternatively, if this latter process occurred at all, one would have to conclude that it happens much faster than we can detect. These results argue against a model in which empty capsids are formed, followed by the uptake of RNA.

The self-assembly of protein subunits by pH-jump could indicate that the reconstitution of the virus is performed through a previous formation of empty capsids which subsequently take up RNA. The fact that in some circumstances the RNA escapes from the virus without disruption of the capsid (Herzog 1976) could lead to the same idea. In fact, both, analytical centrifugation, and neutron scattering prove that this is not the case. The capability of the BMV protein to assemble into capsids in response to pH changes appears to have no major relevance for the BMV morphogenesis. It seems that the protein-protein interactions play a role in the finishing of the virus formation, the protein-RNA interactions being the factor initiating the process.

Acknowledgements. We wish to thank Jean-Marie Bois for the design and construction of the dialysis cell and associated equipment. Roland May and Jim Torbet for their generous help during the neutron experiments. We thank also Bernard Jacrot for encouragement and extensive discussions throughout this project.

References

Abad-Zapatero C, Abdel-Meguid SS, Johnson JE, Leslie AGW, Rayment I, Rossmann MG, Suck D, Tsukihara T (1980) Structure of southern bean mosaic virus at 2.8 Å resolution. Nature 286:33–39

Berthet-Colominas C, Cuillel M, Koch M, Vachette P, Jacrot B (1987) Kinetic study of the self-assembly of brome mosaic virus capsid by X-rays scattering. Eur Biophys J 15:169–178

Cuillel M, Berthet-Colominas C, Krop B, Tardieu A, Vachette P, Jacrot B (1983 a) Self-assembly of brome mosaic virus capsids. Kinetics study using neutron and X-ray solution scattering. J Mol Biol 164:645–650

Cuillel M, Zulauf M, Jacrot B (1983 b) Self-assembly of brome mosaic virus protein into capsids. Initial and final states of aggregation. J Mol Biol 164:589–603

Harrison SC, Olson AJ, Schutt CE, Winkler FK, Bricogne G (1978) Tomato bushy stunt virus at 2.9 Å resolution. Nature 276:368–373

Herzog M (1976) Interactions RNA-protein in a virus having a divided genome: the brome mosaic virus. Thesis in Strassburg University

Ibel K (1976) The neutron small angle camera DII at the high-flux reactor, Grenoble. J Appl Crystallogr 9:296–309

Incardona NL, Kaesberg P (1964) A pH-induced structural change in bromegrass mosaic virus. Biophys J 4:11–21

Incardona NL, McKee S, Flanegan JB (1973) Noncovalent interactions in viruses characterization of their role in the pH and thermally induced conformational changes in bromegrass mosaic virus. Virology 53:204–214

Jacrot B (1976) The study of biological structures by neutron scattering from solution. Rep Prog Phys 39:911–953

Jacrot B, Chauvin C, Witz J (1977) Comparative neutron small-angle scattering study of small spherical RNA viruses. Nature 266:417–421

Kaper JM, Diener TO, Scott HA (1965) Some physical and chemical properties of cucumber mosaic virus (strain Y) and of its isolated ribonucleic acid. Virology 27:54

Kelly JJ, Kaesberg P (1962 a) Preparation of protein subunits from Alfalfa mosaic virus under mild conditions. Biochim Biophys Acta 55:236

Liljas L, Unge T, Jones TA, Fridborg K, Lovgren S, Skoglund U, Strandberg B (1982) Structure of satellite tobacco necrosis virus at 3 Å resolution. J Mol Biol 159:93–108

Pfeiffer P, Hirth L (1974) Aggregation states of brome mosaic virus protein. Virology 61:160–167

Pfeiffer P, Durham ACH (1977) The cation binding associated with structured transitions in bromegrass mosaic virus. Virology 81:419–432

Schneider D, Zulauf M, Schafer R, Franklin RM (1978) Structure and synthesis of a lipid containing bacteriophage. Neutron small angle scattering on bacteriophage PM2. J Mol Biol 124:97–122

Sgro JY, Jacrot B, Chroboczek J (1986) Identification of regions of brome mosaic virus coat protein crosslinked in situ to viral RNA. Eur J Biochem 154:69–76

Vriend G, Verduin BJM, Hemminga MA, Schaafsma TJ (1982) Mobility involved in protein-RNA interaction in spherical plant viruses studied by nuclear magnetic resonance spectroscopy. FEBS Lett 145:49–52

Yamazaki H, Kaesberg P (1963 a) Isolation and characterization of a protein tein subunit of broad bean mottle virus. J Mol Biol 6:465

Yamazaki H, Kaesberg P (1963 b) Degradation of bromegrass mosaic virus with calcium chloride and the isolation of its protein and nucleic acid. J Mol Biol 7:760

Zulauf M (1977) Swelling of brome mosaic virus as studied by intensity fluctuation spectroscopy. J Mol Biol 114:259–266

Zulauf M, Cuillel M, Jacrot B (1981) Neutron and light scattering studies of brome mosaic virus and its protein. In: Chen SH, Chu B, Nossal R (eds) Scattering techniques applied to supramolecular and nonequilibrium systems. Plenum Press, New York